A new guideway design for the HTS Maglev vehicles considering curve negotiation

A new guideway design for the HTS Maglev vehicles considering curve negotiation

Selim Sivrioglu[1], **Ali Suat Yıldız**[2], **Muhammet Islam Bedirbeyoğlu**[3]

[1]Department of Mechanical Engineering, Antalya Bilim University, Antalya-Turkey
[2]Department of Mechanical Engineering, Sivas University of Science and Technology, Turkey
[3]Department of Mechanical Engineering, Gebze Technical University, Turkey

selim.sivrioglu@antalya.edu.tr, suat@sivas.edu.tr, muhammet0islam@gmail.com

Abstract. High-temperature superconducting (HTS) magnetic levitation (maglev) systems have been studied by various research groups regarding both experimental and modelling point of view. However, there exists a trade-off between levitation and guidance forces acting on the vehicle, especially in the case of high-speed curve negotiation. To overcome this trade-off, we proposed a multi-surface permanent magnet guideway (PMG) design, for the small-scale maglev vehicle, in which polarization of the permanent magnets (PM) changing with track segments. The HTS-PM interaction model was constructed by utilizing H-formulation implemented in COMSOL Multiphysics®. The hysteretic levitation and guiding force expressions used in the dynamic simulation have been obtained by a polynomial fit to force-displacement curves obtained by the finite element model built in COMSOL Multiphysics® environment. Also, the damping effect derived from free-fall dynamic tests is incorporated into the model to construct a more realistic simulation model. The effectiveness of the proposed track design has been validated through comparisons with Halbach-derived PMG. Finally, it can be thought that the proposed PMG design is a good candidate for the high-speed operation of a maglev system when the increased levitation and guiding stiffness values are considered.

1. Introduction

HTS maglev vehicles become more prominent in ground transportation systems especially with the technological developments in vacuum insulated cryostats when compared to a maglev vehicle with electromagnetic suspension (EMS) which uses attractive force between vehicle and track, or electrodynamic suspension (EDS) based on repulsive forces. Besides their nature of self-stabilizing levitation characteristics, it has some advantages, such as no mechanical contact, low energy consumption and low noise level.

The electromagnetic relation between bulk material placed in cryostat and PMG have been studied regarding both experimental [1-3] and modelling point of view to optimize levitation and guiding force. The main concern is to achieve maximum force at a minimum material of superconductors and permanent magnets. This can be achieved by optimizing the two major factors: intrinsic properties changing with chemical processes of bulk superconductors and working condition of the vehicle such as cooling heights of the HTS, the vehicle velocity and guideway design [4,5].

For the magnetic guideway design, the Halbach configuration has been studied by many researchers and employed in the experimental test lines [5,6]. Also, a “V” shaped PMG had been used in the UAQ4 bogie system and investigated the effect of the transition curve length on curving performance [7].

To reduce PMG cost, a double-layer Halbach structure which is consisted of NdFeB and ferrite magnets is proposed in [8] and a double-pole Halbach permanent magnet guideway (PMG) was presented to provide a smooth transition to the circular curve segment of the track by modifying the bottom side of the PMG [9]. Also, a new guideway design was constructed by replacing the vertical magnetized PMs in the original Halbach PMG with two oblique magnetized PMs while keeping the PMG cross-sectional area unchanged in [10]. A universal design criterion, regarding levitation height, for the geometric dimension of Halbach PMG is proposed in [11].

Furthermore, in practical application, the vehicle can move in any direction with changing velocity on the prescribed path including curved segments. Therefore, the constructed model should reflect the hysteretic nonlinear behaviour of the HTS-PMG relation. The quasi-static force characteristic gives information for designing the PMG or vehicle model, but for more realistic design, a coupled simulation structure should be built. To predict the levitation characteristics and enhance the performance of the HTS applications, it is necessary to use some modelling tools.

Among these tools, analytic models can be used for simple geometries under certain assumptions [12,13]. For a more complex structure, a numerical model that is derived from Maxwell's equations to describe the interaction between PM and HTS are required. H-formulation based on the magnetic field become a popular tool for simulating the levitation behaviour of HTS due to its computational speed and ease of implementation by using commercial FEM software [5,14-16]. Motivated by these observations, a new PMG structure is proposed to ensure vehicle stability on curved track by improving the vertical and lateral stiffness. This was achieved by using the three surfaces of the HTS effectively with the multi-surface levitation concept.

2. H-Formulation Structure

Maxwell's equations can be solved using the COMSOL built-in module, magnetic field formulation (mfh). In this module, the bulk HTS is modelled as a material with non-linear resistivity obtained by a power law. The non-linear resistivity ρ_{sc} derived from the $E-J$ power-law can be expressed as

$$\rho_{sc} = \frac{E_c}{J_c(B)}\left|\frac{J}{J_c(B)}\right|^{n-1} \tag{1}$$

Here, $J_c(B)$ is the field-dependent critical current density. The critical current density is determined by the magnetic field and a model constant H_0 obtained from experimental measurements [17]. The relationship between the critical current density and magnetic field described as in equation (2)

$$J_c = J_{c_0}\exp\left(-\frac{|H|}{H_0}\right) \tag{2}$$

where H is the magnetic field strength, the levitation force can be calculated by the Lorentz force formula in the form of equation (3)

$$F_{y,x} = l\mu_0\int_S J_z H_{x,y}\,dS \tag{3}$$

Here H_x and H_y are the magnetic field components in $-x$ and $-y$ direction, respectively. The rest of the HTS material parameters used in the simulation, which roughly represent the material properties of YBCO at 77 K are given in Table 1.

Table 1. Parameters of the superconductor.

Symbol	Definition	Value	Unit
M_0	The magnetization of all PM (N35)	8.753×10^5	A/m
E_c	Critical current criterion	1×10^{-4}	V m^{-1}
ρ_{air}	Air resistivity	1	Ω m
μ_0	Air/HTS permeability	$4\pi \times 10^{-7}$	H m^{-1}
n	Power law exponent (1-∞)	21	
J_{c0}	Zero-field critical current density	2.4×10^8	A m^{-2}
H_0	Kim model parameter	0.37	T
l	Model depth	0.2	m
v_{sc}	The moving speed of HTS in cases	1	mm s^{-1}

3. Proposed PMG Structure

In this study, it is assumed that each cryostat is placed in the corner of the HTS maglev vehicle and interacts with PMG as given in Figure 1. The inner sub-figure of Figure 1 indicates the front view of the single cryostat and the PMG. The proposed structure enables the effective use of the side faces of the HTS to levitate the cryostat by the lateral and vertical stiffness effects.

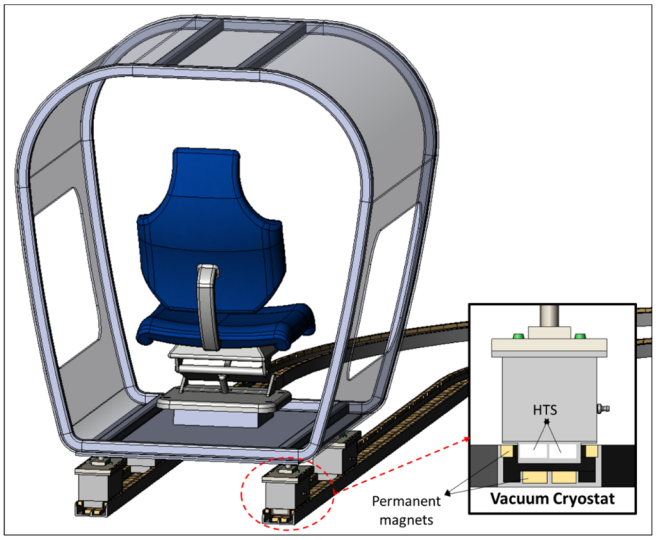

Figure 1. Small-scale maglev vehicle.

The schematic representation model that focused on HTS-PM interaction is given in Figure 2(a) in conjunction with the dimension of PMs. Each dark grey rectangular corresponding to permanent magnets are numbered PM-1 to PM-7. The HTS bulk used in the maglev vehicle has a dimension of 40x40x13 and shown as dotted background in Figure 2. In the simulation study, it is assumed that ten HTS bulk are used for each cryostat. There is a coupled vibratory motion of the lateral and vertical axis when passing through curves. This movement can be treated as two independent single-degree-of-freedom systems in vertical and lateral direction [18]. In the practical vibration of HTS systems, displacement and velocity are time-varying and exhibit minor loops around the initial position. To simulate this dynamic behaviour, the HTS domain was moved towards PMG and then moved away from PMG to investigate the magnetic levitation characteristics of the HTS bulk above the PMG. The direction and sequence of the applied movement to obtain the vertical force characteristic are described with blue arrow and number respectively, in Figure 2(b).

The same procedure was applied in the case of lateral movement as described in Figure 2(c). The PMs placed on both side of PMG provide weighting ability which would be key in terms of switching between lateral and vertical forces. The polarization direction of the PMs placed on the left and right side of the HTS are shown with the bold black arrows as given in Figure 2(d), Figure 2(e) and Figure 2(f). Here, "Case 1" was formed by adding PM-1 and PM-2 which has the polarization shown in Figure 2(d) on the Halbach array with the height of 50 mm and the total length of 100 mm. "Case 2" and "Case 3" was constructed by using the same PM dimension but the different polarization as shown in Figure 2(e) and Figure 2(f), respectively.

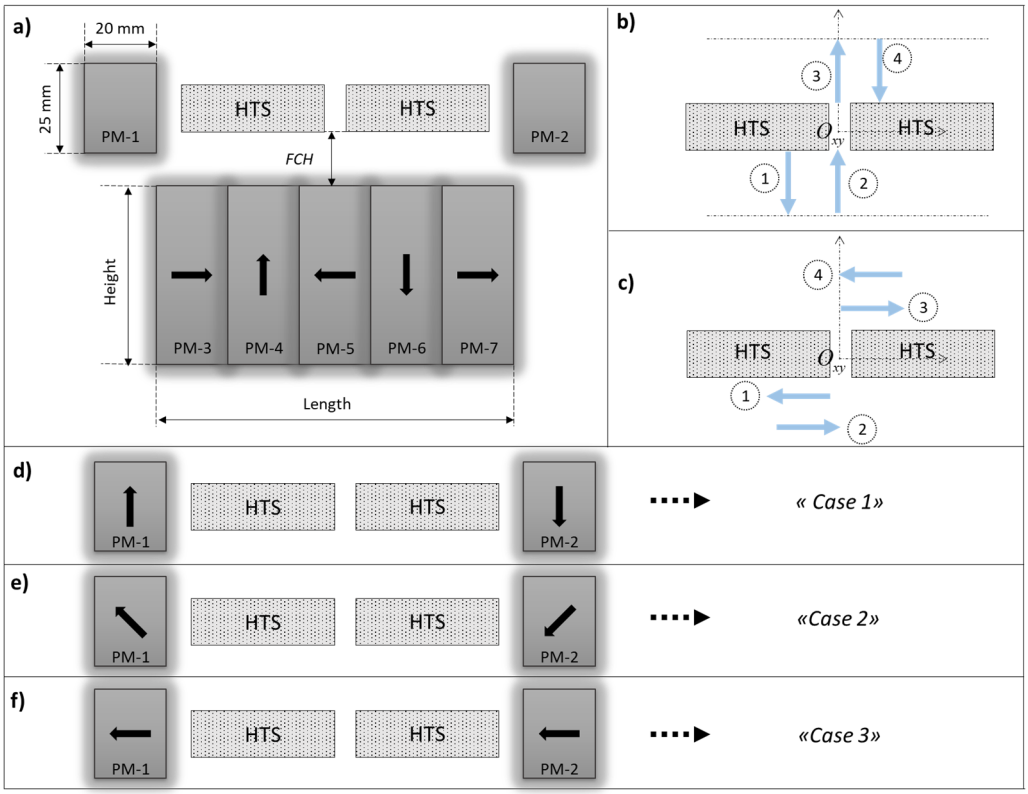

Figure 2. The simplified HTS-PMG interaction model, a) cross-sectional view, b) vertical movement, c) lateral movement, d) side PMs for Case 1, e) side PMs for the Case 2. f) side PMs for the Case 3.

The Halbach array cases without side PMs were selected as reference cases to show that the higher levitation or guiding force can be achieved by the proposed cases. Also, it should be noted that the cross-sectional area of all cases is the same. Halbach H60 indicates an array with the height of 60 mm and total length of 100 mm, Halbach L120 points out the array with the height of 50 mm and total length of 120 mm. As shown in Figure 3, in superconducting levitation systems, a hysteresis effect exists in the loading and relaxing process of the HTS. Here the superconductors were moved 5 mm from its cooling position of 14.2 mm above the track with the loop described in Figure 2(b) and Figure 2(c) at a velocity of 1mm/s. Although the highest levitation force is obtained in the Case 1, it creates the lowest force in terms of guiding. This case is a good choice for the situation in which the guiding has little importance. When the levitation and guiding performance are considered simultaneously, the Case 2 has become prominent. In the present study, a third-order polynomial as given in equation (4) was used to simulate force due to the descent and ascent process of the cryostat. Here, the curve fit given in Figure 3 for the Case 1 also can be considered as an average value of the ascent and descent process.

$$f_{lev,guide} = p_1 z^3 + p_2 z^2 + p_3 z + p_4 \tag{4}$$

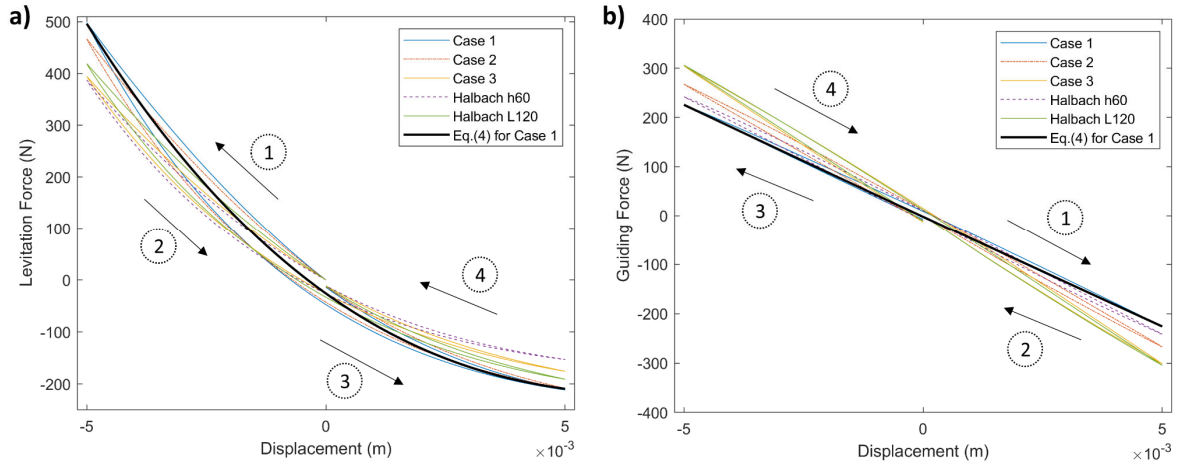

Figure 3. (a) Levitation, (b) Guidance forces of the HTS bulk at the displacement range of ±5 mm.

The produced force as described in equation (3), is the result of the combined effect of both the induced current density inside the HTS domain and the magnetic field. To make this combined effect apparent, the force distribution plot in the HTS domains for a 5 mm displacement are given in Figure 4(a) and Figure 4(b) in the levitation and the guiding direction, respectively. The intensity of the colour is proportional to the distribution of the force density. Here, the Case 3 array appears as the configuration which provides the lowest levitation force because of its weak current penetration. However, by changing the permanent magnet polarization on the side surfaces as in the Case 1, the magnetic flux is compressed between the superconductor and PMG so that higher levitation force can be produced both in the bottom and side surfaces. Also, the intermittent distribution of force on the bottom side of HTS reduces the maximum guiding force in Case 1 and Case 2.

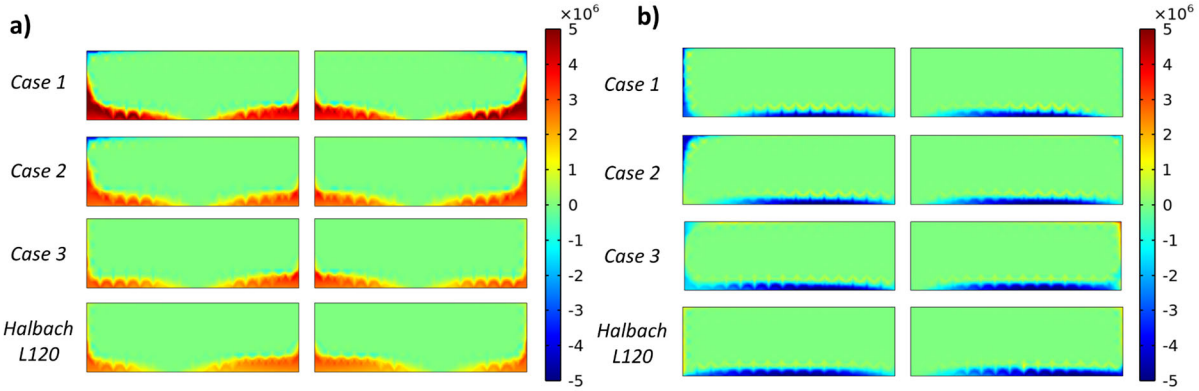

Figure 4. Distribution of the force in the HTS domains: (a) Levitation forces, (b) guidance forces.

As summarized in Table 2, changing the polarization of the PM-1 and PM-2 in Case 1 cause an increase of 22.2% and 15.9% in the levitation force when compared to Halbach H60 and Halbach L120, respectively. Also, the guiding force of Case 3 comes close to that of Halbach L120.

Table 2. Guiding and Levitation force responses of the considered cases.

F_{max} (N)	Case 1	Case 2	Case 3	Halbach H60	Halbach L120
Levitation	498.10	466.98	394.46	387.45	418.92
Guiding	226.42	267.83	305.11	242.30	306.40

4. Determination of the Working Height

The initial field cooling height (FCH) affect the HTS-PMG dynamic response due to the nature of the flux pinning mechanisms. In addition, the damping effect should be determined for the dynamic simulation study. The equation of motion of the maglev system can be defined as,

$$m_{Maglev}\dot{v}_{sc} + cv_{sc} - F_z + F_g = 0 \tag{5}$$

Here v_{sc} is the velocity of the each cryostat, c is the damping coefficient and F_z, F_g are the levitation and gravity forces, respectively. The amount of free fall in the case of the various field-cooling height are given in Figure 5(a). Also, the free vibration curve can be approximated by a damped sine wave, which seems to decrease exponentially as given in Figure 5(b).

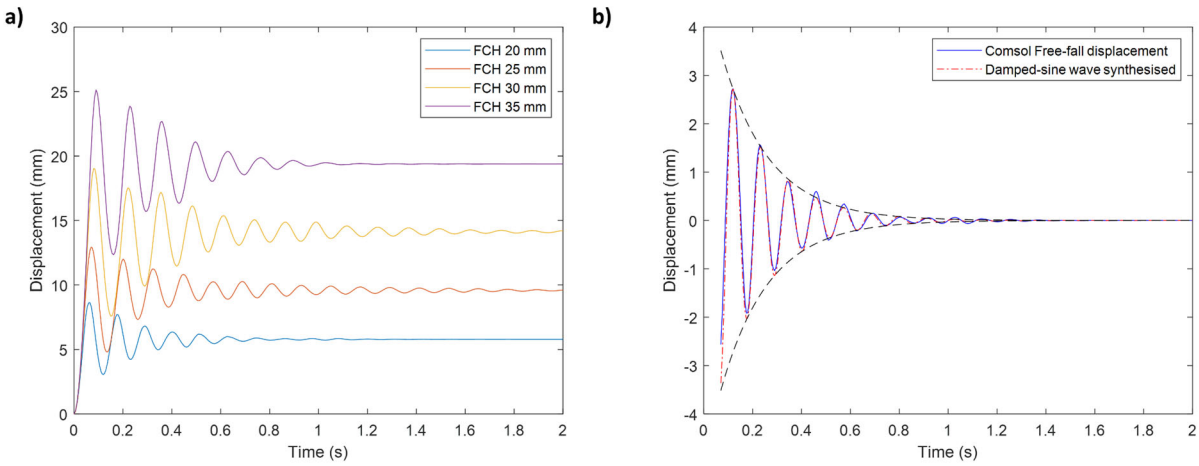

Figure 5. Dynamic response of the HTS levitation system under gravity effect: (a) Effect of the FCH, (b) Dynamic response of the damped sine wave for FCH of 20 mm.

It can be seen in Table 3 that the stiffness tends to increase with the decreasing of the FCH. However, the damping coefficient of the HTS-PM interaction model cannot exhibit a trend. Lower FCH may provide higher stiffness and stability but it should be selected appropriately to ensure the working limits.

Table 3. Damping and stiffness coefficient of the single cryostat at different FCH.

	FCH 20 mm	FCH 25 mm	FCH 30 mm	FCH 35 mm
Linear Damping (N.s/m)	256.6	154.4	166.3	237.5
Linear Stiffness (N/mm)	77.83	67.60	58.76	53.80
Working Height (mm)	14.2	15.4	15.8	15.6

5. Dynamic Performance on Curve

In the simulation study, the mass of the small scale-maglev vehicle is set to 100 kg and guideway irregularities were not considered. The horizontal road profile used to validate the proposed PMG configuration consists of a 50 m straight segment and circular curve series that have a radius of 300 m, 200m and 150 m. Also, a 12 m transition curve is used to enable a gradual transition in lateral acceleration. The superelevation value is selected as 10 mm for the corresponding circular curves. The vehicle speed is kept constant at a value of 15 m/s during the designed route. As seen in Figure 6, the proposed PMG structure provides better lateral stability when compared to a conventional Halbach array

of the same cross-sectional area. Also, it is noted that the decrement in both lateral and vertical direction tends to be higher with the smaller curve radius. The same trend can be preserved in the vertical displacement of the vehicle's centre of gravity (COG). The Case 2 is selected as the proposed case because of providing higher force in both levitation and guiding and labelled as "Proposed" in the legend. It can be seen in Figure 6 that the superelevation used for reducing the centrifugal effect cause oscillations that occurs when the vehicle entered and left the circular curve. Also, the effectiveness of the proposed array becomes more prominent as the radius of the curve decreased. Also, the proposed PMG structure provides lower displacement in the vertical and lateral direction as in the roll angle of the vehicle.

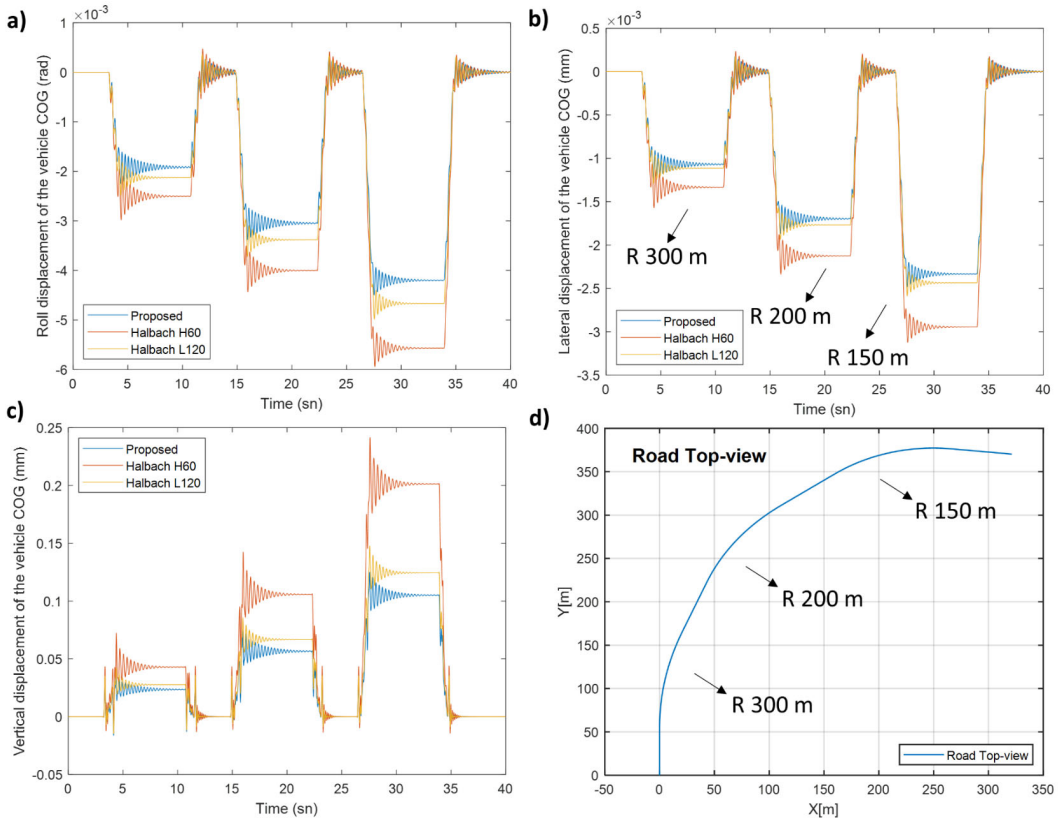

Figure 6. Curving performance, (a) Roll displacement, (b) Lateral displacement, (c) Vertical displacement, (d) Top-view of the guideway.

6. Conclusions

In this article, a simulation method based on H-formulation was applied to the HTS maglev vehicle that comprises the multi-surface levitation concept. The attained higher force values with the proposed array provides better stability when compared to Halbach array cases. This improvement also leads to better resistance to centrifugal force, especially while the vehicle passes through the small curve. The vertical displacement and the roll angle of the vehicle were decreased by adding side PMs with proper polarization, this improvement provides higher carrying capacity and sufficient anti-overturning capacity. Also, the total amount of magnet that refers to the fabrication cost of the maglev systems can be decreased with the proposed PMG structure.

Acknowledgments

This research study is supported by The Scientific and Technological Research Council of Turkey under the support program of 1001 with project number 217M320.

References

[1] Sotelo G G, Dias D H N, de Andrade R and Stephan R M 2011 Tests on a superconductor linear magnetic bearing of a full-scale MagLev vehicle *IEEE Trans. Appl. Supercond.* **21** 1464–8
[2] Schultz L, deHaas O, Verges P, Beyer C, Rohlig S, Olsen H, Kuhn L, Berger D, Noteboom U and Funk U 2005 Superconductively levitated transport system—the SupraTrans project *IEEE Trans. Appl. Supercond.* **15** 2301–5
[3] Wang J, Wang S, Zeng Y, Huang H, Luo F, Xu Z, Tang Q, Lin G, Zhang C, Ren Z, Zhao G, Zhu D, Wang S, Jiang H, Zhu M, Deng C, Hu P, Li C, Liu F, Lian J, Wang X, Wang L, Shen X and Dong X 2002 The first man-loading high temperature superconducting Maglev test vehicle in the world *Physica C Supercond.* **378–381** 809–14
[4] Li H, Deng Z, Ke Z, Yu J, Ma S and Zheng J 2020 Curve negotiation performance of high-temperature superconducting maglev based on guidance force experiments and dynamic simulations *IEEE Trans. Appl. Supercond.* **30** 1–11
[5] Huang H, Zheng J, Liao H, Hong Y, Li H and Deng Z 2019 Effect laws of different factors on levitation characteristics of high-Tc superconducting maglev system with numerical solutions *J. Supercond. Nov. Magn.* **32** 2351–8
[6] Sotelo G G, de Andrade R, Dias D H N, Ferreira A C, Costa F, Machado O J, de Oliveira R A H, Santos M D A and Stephan R M 2013 Tests with one module of the Brazilian maglev-cobra vehicle *IEEE Trans. Appl. Supercond.* **23** 3601204–3601204
[7] Deng Z, Zhang W, Zheng J, Ren Y, Jiang D, Zheng X, Zhang J, Gao P, Lin Q, Song B and Deng C 2016 A high-temperature superconducting maglev ring test line developed in Chengdu, China *IEEE Trans. Appl. Supercond.* **26** 1–8
[8] Alaggio R, Carpenito A, D'Ovidio G and Sebastiani D 2018 Transition curve effect on lateral vibration of superconducting experimental maglev bogie: A nonlinear dynamic approach *IEEE Transactions on Applied Superconductivity* **28**
[9] Sun R, Zheng J, Zheng B, Qian N, Li J and Deng Z 2018 New magnetic rails with double-layer Halbach structure by employing NdFeB and ferrite magnets for HTS maglev *J. Magn. Magn. Mater.* **445** 44–8
[10] Lei W, Qian N, Zheng J, Huang H, Zhang Y and Deng Z 2017 Magnetic superelevation design of Halbach permanent magnet guideway for high-temperature superconducting maglev *Physica C Supercond.* **538** 1–5
[11] Deng Z, Zhang W, Chen Y, Yang X, Xia C and Zheng J 2020 Optimization study of the Halbach permanent magnetic guideway for high temperature superconducting magnetic levitation *Supercond. Sci. Technol.* **33** 034009
[12] Werfel F N, Floegel-Delor U, Rothfeld R, Riedel T, Schirrmeister P and Koenig R 2016 Experiments of superconducting maglev ground transportation *IEEE Trans. Appl. Supercond.* **26** 1–5
[13] Sivrioglu S and Cinar Y 2007 Levitation analysis of a ring shaped permanent magnet–high temperature superconductor vertical bearing system *Supercond. Sci. Technol.* **20** 559–63
[14] Prigozhin L 1997 Analysis of critical-state problems in type-II superconductivity *IEEE Trans. Appl. Supercond.* **7** 3866–73
[15] Quéval L, Liu K, Yang W, Zermeño V M R and Ma G 2018 Superconducting magnetic bearings simulation using an H-formulation finite element model *Supercond. Sci. Technol.* **31** 084001
[16] Naseh M and Heydari H 2017 Analytical method for levitation force calculation of radial HTS magnetic bearings *IET electr. power appl.* **11** 369–77
[17] Sass F, Sotelo G G, Junior R de A and Sirois F 2015 H-formulation for simulating levitation forces acting on HTS bulks and stacks of 2G coated conductors *Supercond. Sci. Technol.* **28** 125012
[18] Liu L and Wang J 2014 Vibrational Properties of High-Tc Superconductors Levitated Above a Bipolar Permanent Magnetic Guideway *Journal of Low Temperature Physics* **175**